196

Reprinted from

Journal of Biomolecular NMR

Journal of Biomolecular NMR, 3 (1993) 715–720
ESCOM

J-Bio NMR 162

Minimizing the effects of radio-frequency heating in multidimensional NMR experiments

Andy C. Wang and Ad Bax

Laboratory of Chemical Physics, National Institute of Diabetes and Digestive and Kidney Diseases, National Institutes of Health, Bethesda, MD 20892, U.S.A.

Received 24 August 1993
Accepted 15 September 1993

Keywords: Radio-frequency heating; Line-shape distortion; Multidimensional NMR; Temperature; Decoupling; Isotropic mixing

ESCOM

Journal of Biomolecular NMR, 3 (1993) 715–720
ESCOM

J-Bio NMR 162

Minimizing the effects of radio-frequency heating in multidimensional NMR experiments

Andy C. Wang and Ad Bax

Laboratory of Chemical Physics, National Institute of Diabetes and Digestive and Kidney Diseases, National Institutes of Health, Bethesda, MD 20892, U.S.A.

Received 24 August 1993
Accepted 15 September 1993

Keywords: Radio-frequency heating; Line-shape distortion; Multidimensional NMR; Temperature; Decoupling; Isotropic mixing

SUMMARY

Application of radio-frequency power in multidimensional NMR experiments can significantly increase the sample temperature compared to that of the surrounding gas flow. Radio-frequency heating effects become more severe at higher magnetic field strengths and ionic strengths. The effects are particularly noticeable for experiments that utilize ^{1}H and/or ^{13}C isotropic mixing and broadband decoupling. If radio-frequency power is applied during the systematically increasing evolution period t_1, the sample temperature can change with t_1 and thereby cause line-shape distortions. Such distortions are easily avoided by ensuring that the average radio-frequency power remains constant during the entire experiment.

Radio-frequency (RF) heating effects associated with ^{1}H decoupling in ^{13}C NMR have long been recognized (Led and Petersen, 1978; Alderman and Grant, 1979; Bock et al., 1980; Lewis et al., 1988) and, in fact, helped drive the development of highly efficient composite-pulse decoupling schemes for broadband ^{1}H decoupling (Levitt and Freeman, 1981; Waugh, 1982; Shaka et al., 1985). Many new triple-resonance experiments for the study of isotopically enriched proteins also require substantial amounts of ^{1}H, ^{13}C and ^{15}N irradiation. In particular, those which rely on isotropic mixing of ^{1}H or ^{13}C magnetization (Braunschweiler and Ernst, 1983; Bax and Davis, 1985, Shaka et al., 1988; Bax et al., 1990; Fesik et al., 1990) and on heteronuclear cross-polarization (Bearden and Brown, 1989; Zuiderweg, 1990; Ernst et al., 1991; Morris and Gibbs, 1991) can cause significant sample heating. On commercial spectrometers the sample temperature itself is generally not regulated: The temperature control unit merely controls the temperature of the gas that flows past the sample. Depending on probe design, the thermocouple is positioned in the gas stream either before or after it passes by the sample, or the thermocouple may sense the temperature of a mixture of gas which has and has not passed by the sample. In each case, RF irradiation will increase the sample temperature relative to the regulated temperature of the gas, albeit to different degrees. As a consequence, when different experiments are recorded at the same 'set'

temperature, the actual sample temperatures can be substantially different. The resulting changes in chemical shift are frequently nonuniform and can seriously hamper the effectiveness of automated resonance-assignment procedures.

Even if the solute chemical shifts do not vary much with temperature, sample heating can still cause problems as the HDO resonance, used for the field/frequency lock, has a strong temperature dependence (ca. −0.01 ppm/°C). In particular, when the average RF power deposited in the sample depends on the duration of the evolution period(s), the sample temperature will vary within a single experiment, resulting in line-shape distortions. As described below, such distortions can be avoided by using a simple compensation procedure.

Sample heating originates primarily from the interaction between the electric component of the RF field and the electric dipole moments of the solvent and solute molecules and the ions surrounded by their atmosphere of opposite charge. At a given strength of the electric component of the RF field, the absorbed energy increases approximately with the square of the frequency (Led and Petersen, 1978; Gadian and Robinson, 1979; Bock et al., 1980). The actual amount of RF energy absorbed by the sample at a given strength of the magnetic component (i.e., the RF field component that interacts with the nuclear magnetic moment) depends strongly on the ratio of the magnetic and electric components of the RF field within the sample and can therefore be optimized by suitable probe design (Alderman and Grant, 1979; Hoult and Lauterbur, 1979). In addition to coil design, frequency, power level, solvent, solute and ionic strength, the degree of sample heating also depends on the flow rate of the gas and the diameter of the sample tube.

First, we describe a simple method for determining the change in sample temperature caused by RF irradiation. The method is applied to two samples of different ionic strengths, each in a 5 mm sample tube, using a Bruker triple-resonance 600 MHz probehead and an airflow of 350 l/h. The probehead contains an inner coil tuned for ^{1}H and ^{2}H and an outer coil tuned for ^{13}C and ^{15}N. The first sample contains 6 mM sucrose and 0.1 mM 3-(trimethylsilyl)propionic-2,2,3,3-d_4 (TSP) dissolved in D_2O. The second sample is identical except for an additional 200 mM NaCl. The degree of sample heating is monitored by measuring the difference between the TSP and the HDO resonances. Since the spectrometer is field-frequency locked on the deuterium resonance of HDO, the HDO proton resonance does not shift noticeably with increasing temperature; instead a downfield shift is observed for the rest of the NMR spectrum. The chemical-shift difference between TSP and HDO decreases by 0.01 ppm/°C and is therefore a convenient and accurate monitor for the internal sample temperature. For ^{1}H, each FID (of 680 ms) was preceded by a 145 ms burst of RF power, applied far off-resonance, and was followed by a 174-ms relaxation delay prior to the recording of the next FID. The ^{1}H power level in Table 1 has been corrected for this 14.5% duty cycle. For ^{13}C and ^{15}N, irradiation can be applied continuously as it does not affect the observed proton spectrum (apart from the change in temperature). For all three frequencies, the actual recording of the proton spectrum was preceded by a 5-min period during which the experiment was repeated continuously (dummy scans). The applied power level was monitored with a Bird Model 4391 Watt meter. Sample heating resulting from irradiation at the ^{1}H, ^{13}C and ^{15}N frequencies is summarized in Table 1.

As is clear from Table 1, the degree of heating depends strongly on the ionic strength, particularly for ^{1}H irradiation. For a given ^{1}H RF field strength, the heating increases more than eightfold when the ionic strength is increased from near-zero to 200 mM NaCl. For a HOHAHA experiment using a 50-ms mixing period with a 10-kHz RF field and a repetition rate of 1 s^{-1}, the sample tempera-

ture increases by 0.4 and 3 °C for the no-salt and the 200 mM NaCl samples, respectively. For a HCCH-TOCSY experiment (Bax et al., 1990) using a 25-ms ^{13}C mixing period with a 7.5-kHz RF field, and 50 ms ^{13}C decoupling during data acquisition with a 5-kHz RF field at a 1 s^{-1} repetition rate, the sample temperature increases by 1.3 and 2.5 °C for the low- and high-salt samples, respectively. For ^{15}N irradiation, we find heating effects to be negligible for all practical purposes.

The amounts of RF heating quoted above are for a constant repetition rate of the pulse sequence. Except for constant-time experiments, the repetition rate decreases when the evolution period increases. During the experiment, therefore, the amount of RF power applied to the sample changes and causes a concomitant change in sample temperature. If no RF irradiation is used during the evolution period, the heating effect will decrease with increasing t_1. However, if decoupling is applied during t_1, the sample temperature can increase with increasing t_1. Consider, for example, the pulse sequence of Fig. 1 which correlates H^N with ^{15}N and uses broadband ^{13}C decoupling to eliminate ^{15}N–^{13}C J-couplings in the ^{15}N dimension. When high resolution in the ^{15}N dimension is required and correspondingly long t_1 durations are needed, the sample temperature at the long t_1 durations can be substantially higher than at the short t_1 durations.

The result of the above-mentioned HSQC experiment is demonstrated for a 1.5-mM sample of $^{13}C/^{15}N$ doubly labeled calmodulin (CaM) complexed with a 26-residue peptide fragment of skeletal muscle myosin light-chain kinase (M13) in 95% H_2O/5% D_2O, 100 mM KCl, 6.8 mM $CaCl_2$, at pH 6.8. Spectra were recorded on a Bruker AMX 600 spectrometer operating at 35 °C. Figure 2A shows the HSQC spectrum collected using the pulse sequence sketched in Fig. 1, but without ^{13}C CW irradiation during t_c. The delay time between scans, including a 55-ms t_2 acquisition period, was 1 s. The correlations for many of the amides in Fig. 2A have a horizontal tear-drop shape, which is more pronounced for some resonances than for others and which results from the higher temperatures at longer t_1 durations. As is well known and frequently utilized in peptide studies, H^N chemical shifts exhibit a significant temperature dependence (~ −0.003 to −0.008 ppm/°C) which partially offsets the change in resonance frequency caused by the temperature dependence of the HDO resonance. H^N resonances with a strong temperature dependence therefore show the least line-shape distortion in the ^{15}N–H^N HSQC spectrum of Fig. 2A.

TABLE I

RF FIELD STRENGTH (γB_1) AND CORRESPONDING TEMPERATURE INCREASE (ΔT) FOR A TRIPLE-RESONANCE 600 MHz PROBEHEAD[a]

Nucleus	No salt[b]		200 mM NaCl[c]	
	γB_1 (kHz/W)[d]	ΔT (°C/W)[e]	γB_1 (kHz/W)[d]	ΔT (°C/W)[e]
^1H	9.4	6.7	6.8	29
^{13}C	1.8	1.6	1.8	3.0
^{15}N	0.5	0.07	0.5	0.1

[a] The temperature control unit is operating at a 'set' temperature of 35 °C.

[b] 6 mM sucrose and 0.1 mM TSP in D_2O (400 µl).

[c] 200 mM NaCl, 6 mM sucrose and 0.1 mM TSP in D_2O (400 µl).

[d] Derived from its value measured at 10 W RF power, where the Watt meter is most accurate.

[e] Calculated from a least-squares fit of the chemical-shift difference between TSP and HDO at several different power levels.

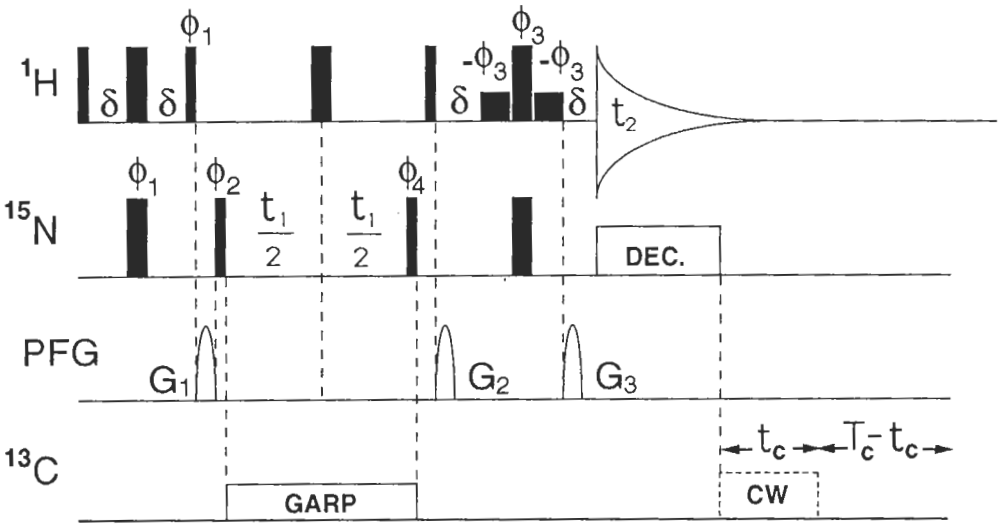

Fig. 1. Pulse scheme for the ^1H–^{15}N HSQC correlation experiment (Bodenhausen and Ruben, 1980) with ^{13}C decoupling during t_1. Non-temperature-compensated experiments were performed without the ^{13}C CW pulse. Constant-temperature experiments, on the other hand, employed additional ^{13}C CW irradiation. Narrow and wide pulses correspond to 90° and 180° flip angles, respectively. Water suppression is accomplished with low-power (274 Hz) $90°_{-\phi 3}$ pulses surrounding the $180°_{\phi 3}$ pulse (Piotto et al., 1992). Pulses without a phase symbol are applied along the x-axis. The ^1H carrier is set at the H_2O frequency, the ^{15}N carrier is at 116.5 ppm and the ^{13}C carrier is positioned halfway between the C^{α} and CO resonances, at 115 ppm. ^{13}C decoupling is applied with a 5-kHz RF field using GARP modulation (Shaka et al., 1985). The applied pulsed field gradients, G_1, G_2 and G_3 all have a sine-bell shaped amplitude profile with a gradient strength of 10 G/cm at the center of the sine bell and durations of 2.6 ms (G_1) and 600 μs (G_2, G_3). Phase cycling is as follows: ϕ_1 = y,−y; ϕ_2 = x,x,−x,−x; ϕ_3 = x; ϕ_4 = 4(x),4(−x), and Acq = x,2(−x),2(x),2(−x),x. The duration t_c is given by $t_c = [1 - (t_1/t_{1max})]\, T_c$, with T_c = 100 ms, t_{1max} = 200 ms, P_{dec} = 7.6 W, P_{comp} = 12.7 W and a recovery delay of 1 s.

The t_1 dependence of the sample temperature can be eliminated by keeping the average decoupling power constant throughout the course of the experiment. This is achieved by inserting a duration, t_c, of high-power ^{13}C decoupling which becomes progressively shorter with increasing t_1 (Fig. 1). Using a 5-kHz (7.6 W) ^{13}C decoupling field during t_1, the average ^{13}C decoupling power for the noncompensated experiment is negligible for short t_1 durations, but steadily increases to 1.3 W when the t_1 duration reaches 200 ms. In the compensated experiment, however, the average ^{13}C decoupling power is maintained at 1.3 W throughout the entire experiment and, hence, the sample temperature remains constant. The duration and power of the RF irradiation for temperature compensation are adjusted to satisfy the following relationship:

$$\frac{P_{dec}t_1 + P_{comp}t_c}{t_1 + T_d} = \frac{P_{dec}t_{1max}}{t_{1max} + T_d} \tag{1a}$$

where P_{dec} and P_{comp} are the ^{13}C decoupling power levels applied during ^{15}N evolution and temperature compensation, respectively, t_{1max} is the maximum t_1 duration used and T_d is the total duration of a single scan for $t_1 = 0$, including the relaxation delay. The duration t_c lies between 0 and T_c, with T_c given by

$$T_c = \frac{t_{1max}\, T_d}{t_{1max} + T_d} \times \frac{P_{dec}}{P_{comp}} \tag{1b}$$

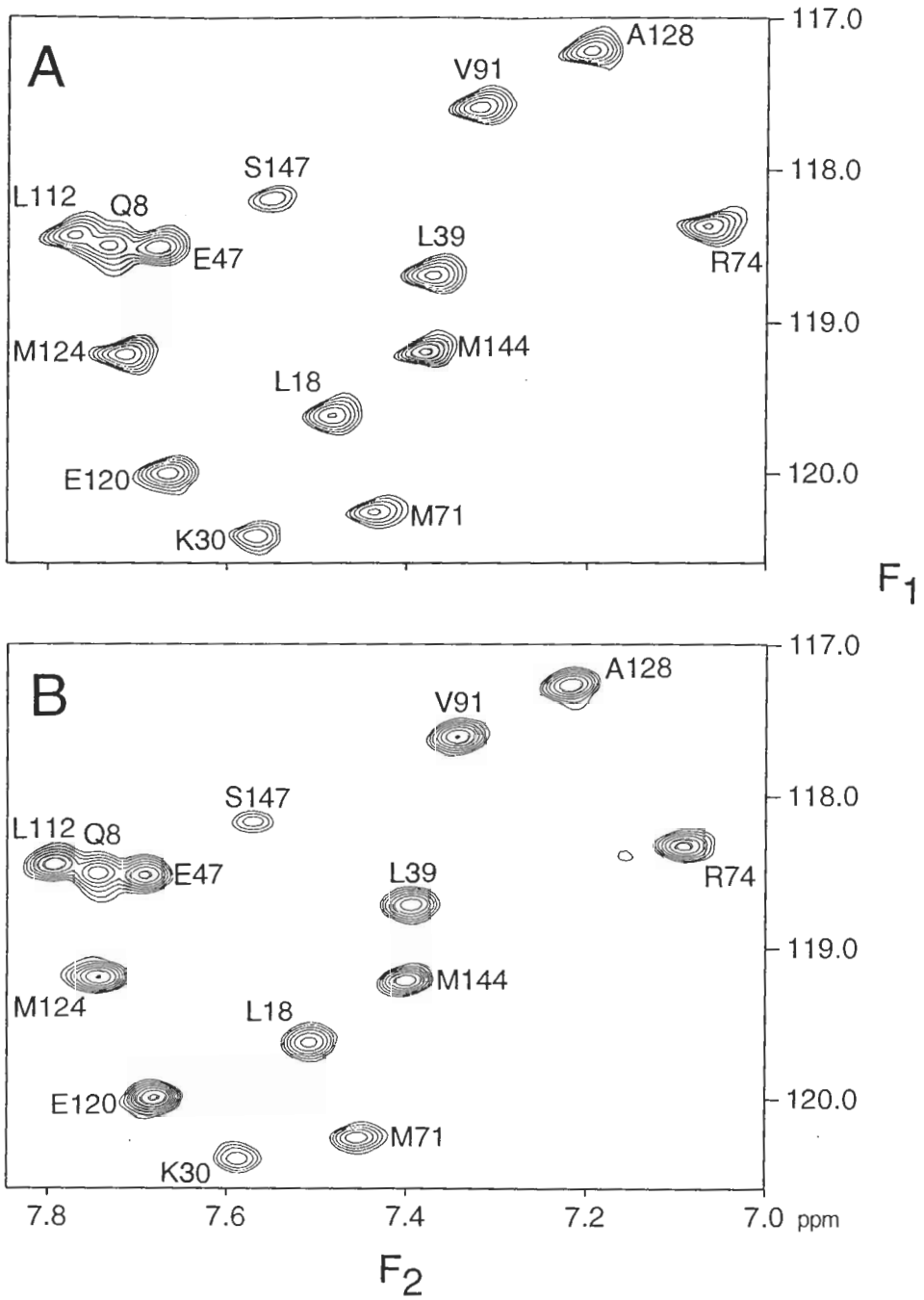

Fig. 2. Small regions of the ^{1}H–^{15}N HSQC spectra of CaM–M13, uniformly enriched in ^{13}C and ^{15}N. The data were collected using the pulse sequence of Fig. 1, (A) without and (B) with ^{13}C CW irradiation during the period t_c. Assignments are taken from Ikura et al. (1991).

Figure 2B shows the effectiveness of the temperature compensation scheme for the HSQC spectrum of the CaM–M13 complex. For the intermediate ionic strength of this particular sample, the temperature increase is ~3 °C over the set temperature of 35 °C.

As discussed above, RF irradiation in homo- and heteronuclear multidimensional NMR experiments not only causes the sample temperature to become considerably higher than the set temperature but, more importantly, can also cause the sample temperature to gradually change during the course of a single experiment. Experiments which require very high resolution and for which the average RF power applied to the sample varies significantly with t_1 will benefit from additional, temperature-compensating, RF irradiation applied in the manner described above. It is important that the additional RF irradiation does not interfere with relaxation processes during the delay between scans. That is, for most heteronuclear experiments the compensating irradiation is preferably applied on the ^{13}C channel, or for homonuclear experiments with a '^{1}H-only' probe it should be applied very far (> 100 kHz) off-resonance.

ACKNOWLEDGEMENTS

We thank Stephan Grzesiek and Geerten Vuister for valuable discussions and James Ernst for drafting Fig. 1. ACW is the recipient of an American Cancer Society postdoctoral fellowship (PF-4030). This work was supported by the AIDS Targeted Anti-Viral Program of the Office of the Director of the National Institutes of Health.

REFERENCES

Alderman, D.W. and Grant, D.M. (1979) *J. Magn. Reson.*, **36**, 447–451.
Bax, A. and Davis, D.G. (1985) *J. Magn. Reson.*, **65**, 355–360.
Bax, A., Clore, G.M. and Gronenborn, A.M. (1990) *J. Magn. Reson.*, **88**, 425–431.
Bearden, D.W. and Brown, L.R. (1989) *Chem. Phys. Lett.*, **163**, 432–436.
Bock, K., Meyer, B. and Vignon, M. (1980) *J. Magn. Reson.*, **38**, 545–551.
Bodenhausen, G. and Ruben, D.J. (1980) *Chem. Phys. Lett.*, **69**, 185–189.
Braunschweiler, L. and Ernst, R.R. (1983) *J. Magn. Reson.*, **53**, 521–528.
Ernst, M., Griesinger, C., Ernst, R.R. and Bermel, W. (1991) *Mol. Phys.*, **74**, 219–252.
Fesik, S.W., Eaton, H.L., Olejniczak, E.T., Zuiderweg, E.R.P., McIntosh, L.P. and Dahlquist, F.W. (1990) *J. Am. Chem. Soc.*, **112**, 886–888.
Gadian, D.G. and Robinson, F.N.H. (1979) *J. Magn. Reson.*, **34**, 449–455.
Hoult, D.I. and Lauterbur, P.C. (1979) *J. Magn. Reson.*, **34**, 425–433.
Ikura, M., Kay, L.E., Krinks, M. and Bax, A. (1991) *Biochemistry*, **30**, 5498–5504.
Led, J.J. and Petersen, S.B. (1978) *J. Magn. Reson.*, **32**, I–17.
Levitt, M.H. and Freeman, R. (1981) *J. Magn. Reson.*, **43**, 502–507.
Lewis, J.S., Tomchuck, E. and Bock, E. (1988) *J. Magn. Reson.*, **78**, 321–326.
Morris, G.A. and Gibbs, A. (1991) *J. Magn. Reson.*, **91**, 444–449.
Piotto, M., Saudek, V. and Sklenar, V. (1992) *J. Biomol. NMR*, **2**, 661–665.
Shaka, A.J., Barker, P.B. and Freeman, R. (1985) *J. Magn. Reson.*, **64**, 547–552.
Shaka, A.J., Lee, C.J. and Pines, A. (1988) *J. Magn. Reson.*, **77**, 274–293.
Waugh, J.S. (1982) *J. Magn. Reson.*, **50**, 30–49.
Zuiderweg, E.R.P. (1990) *J. Magn. Reson.*, **89**, 533–542.